16th World Conference on Earthquake, 16WCEE 2017

Santiago Chile, January 9th to 13th 2017

Paper N° 602

Registration Code: S-S1461333221

STATE-OF-ART STABILITY ASSESSMENT OF BUCKLING-RESTRAINED BRACES INCLUDING CONNECTIONS

T. Takeuchi(1), R. Matsui(2), B. Sitler(3), G. MacRae(4)

(1) Professor, Tokyo Institute of Technology, ttoru@arch.titech.ac.jp
(2) Assistant Professor, Tokyo Institute of Technology, Matsui.r.aa@m.titech.ac.jp
(3) Graduate student, Tokyo Institute of Technology,
(4) Associate Professor, University of Canterbury,

Abstract

Buckling-restrained braces (BRBs), developed in the late 1980's in Japan, are now widely used as ductile seismic-resistant and energy dissipating structural members in seismic regions such as the US, Taiwan, China and NZ. They are expected to exhibit stable hysteresis when subjected to in-plane cyclic axial loading, as described in the seismic provisions of AIJ 2009 and AISC 341. However, several recent studies have highlighted the risk of global BRB buckling induced by plastic hinging at the restrainer end prior to core yielding and subsequent connection instability. Various equations evaluating this stability limit have been proposed, but the relationship among these criteria is not clear. This paper reviews and compares these equations, introduces a unified concept and proposes a simplified approach for practical design.

Keywords: Buckling-restrained Braces, Out-of-plane stability, Connections, Buckling

1. Introduction

Buckling-restrained braces (BRBs) developed in the late 1980's in Japan [1], are now widely used as ductile seismic-resistant and energy dissipating structural members in seismic regions around the world. They are expected to exhibit stable hysteresis when subjected to cyclic axial loading, as described in the seismic provisions of AIJ 2009, 2012 [2,3] and AISC 341 [4]. However, several recent studies have highlighted the risk of global BRB buckling induced by plastic hinging at the restrainer end prior to core yielding and subsequent connection instability (Fig.1). Wigle et al. [6] discussed the effect of connections on BRB performance, and Lin, Tsai et al. [7] reported the phenomenon of global buckling related to connection failure in BRB frame tests. To account for this mechanism, various stability limit criteria have been proposed. Tsai, Nakamura et al. [8]

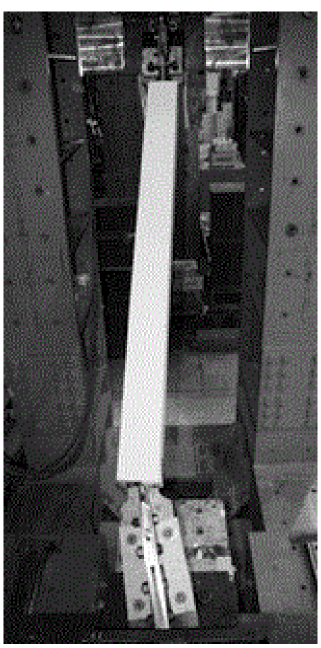

Fig. 1 – Global buckling of BRB including connections

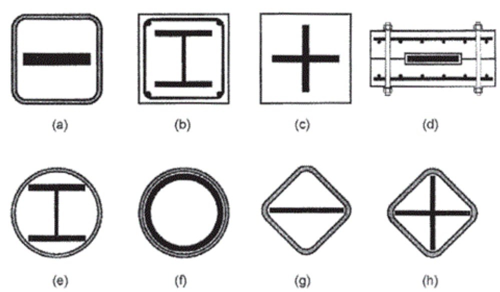

Fig. 2 – Typical BRB sections

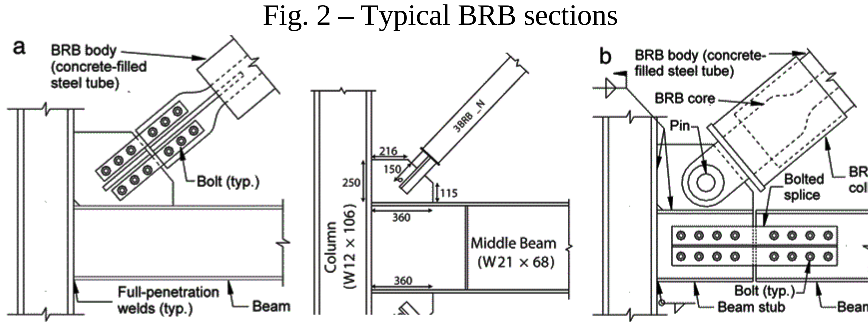

(a) Bolted connection[6] (b) Welded connection[7] (c) Pinned connection[8]
Fig. 3 – Typical BRB's connections

suggested evaluating BRB connection buckling strength by Euler buckling, taking the equivalent length as twice the connection length. However, the theoretical basis is not clearly explained. Koetaka et al. [9] discussed the conditions under which bending-moment transfer capacity at the restrainer ends is lost, assuming full fixity at the gusset base. Okazaki, Hikino et al. [10] proposed simplified criteria using the same assumptions as Koetaka et al. Takeuchi et al. [11] discussed the stability requirements for BRBs including the effects of bending-moment transfer capacity at the restrainer ends, connection zone flexural stiffness, gusset and adjacent framing rotational stiffness, and out-of-plane drift due to the transverse component of ground motion. A simple set of equations was proposed for both the one-way configuration with symmetric boundary conditions and the chevron configuration [12]. This paper reviews and compares these equations and proposes a simplified approach for practical design.

2. BRB configurations

Various BRB cross sections are shown in Fig.2, and some typical connections are shown in Fig.3. Bolted connections are commonly used to enable braces to be replaced following a severe earthquake. Welded connections produce a compact connection, while pinned connections are used to avoid bending moment transfer. In pinned connections, tight tolerances and precise alignment between the pin and hole is required to avoid slack and the resultant pinched hysteresis shape. Although bolted connections are easily replaceable, global stability tends to become the governing design criteria.

Common gusset plate types used for BRB connections are shown in Fig.4. Type A is popular in the US and NZ, but out-of-plane stiffness is low. Those with full depth stiffeners, Types B and C, are used in Japan, and produce relatively high out-of-plane stiffness. Typical BRB framing configurations are shown in Fig. 5, including the (a) one-way configuration with symmetry boundary conditions and (b) chevron configuration with a reduced out-of-plane stiffness at the upper (beam) end.

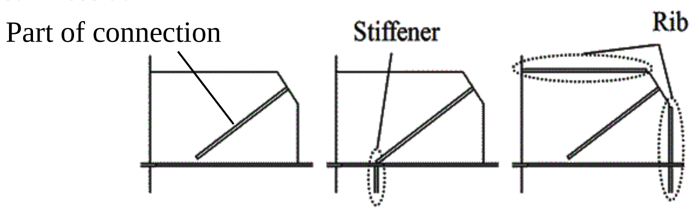

Type A Type B Type C

(a) low stiffness (b) high stiffness

Fig. 4 – Gusset plate types and out-of-plane stiffness[11]

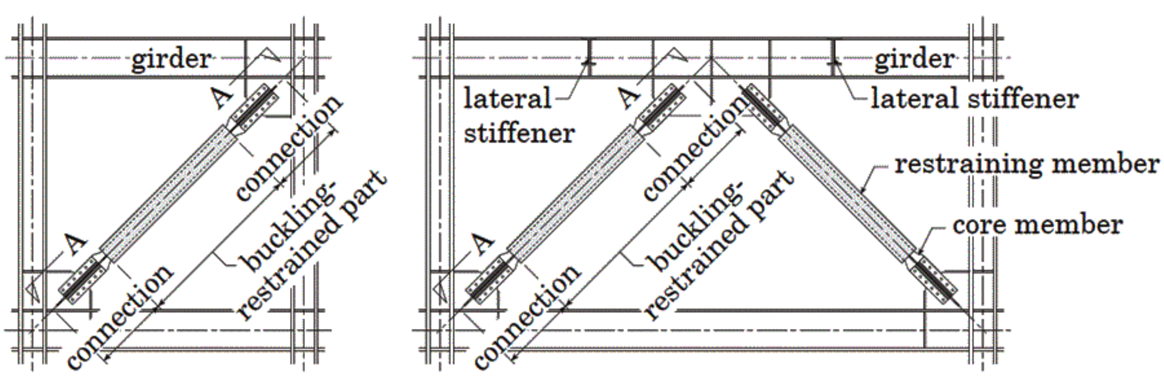

(a) One-way (b) Chevron

Fig. 5 – BRB configurations in frame[9]

3. Tsai and Nakamura's proposal (2002)

One of the earliest design criteria for out-of-plane stability was proposed by Tsai, Nakamura et al. [8], designing the connection for Euler buckling and taking an equivalent length of twice the restrainer end to beam/column centroid length as shown in Fig.6. This method is introduced in the text by Bruneau et al. [13]. It assumes the gusset plate ends to be rotationally rigid and the restrainer end to be a pin, idealizing the connection as a cantilever. However, neither a rigorous theoretical basis, nor detailed explanation is provided.

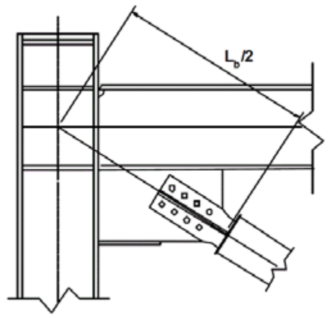

Fig. 6 – Tsai and Nakamura's proposal[8]

4. Koetaka and Inoue's proposal (2008)

Koetaka, Kinoshita, Inoue et al. [9] discussed stability conditions for a BRB in the chevron configuration, including a rotational and horizontal sway spring at the upper (beam) connection as shown in Fig.7. In this model, bending-moment transfer capacity at the restrainer ends is lost and modelled as pin, while the lower gusset plate end is estimated as rotationally rigid. $r_J EI_B$ is the bending stiffness at connections, taken as a percentage of the restrainer flexural stiffness in the direction under consideration and defined in [9].

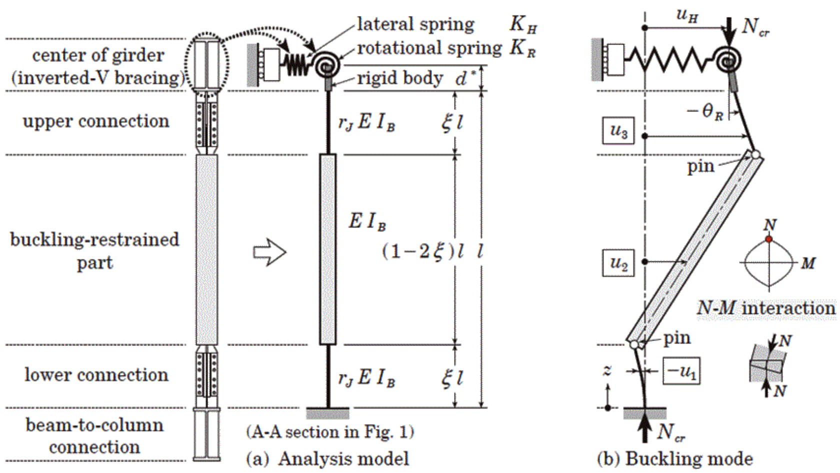

Fig. 7 – Koetaka and Inoue's model[9]

The stability limit is defined as a combination of sway and rotational buckling at the upper (beam) connection. When the upper connection is braced by a fixed secondary beam or by fly bracing and slab, both the rotational and horizontal springs, K_R and K_H, respectively, are large and the elastic buckling strength is defined by:

$$N_{cr} = \frac{\pi^2 (1-2\xi) r_J EI_B}{(2\xi L_0)^2} \tag{1}$$

When a perpendicular secondary beam restrains the sway component, but offers insufficient rotational stiffness K_R to provide full restraint, the stability limit is evaluated by:

$$N_{cr} = \frac{(1-2\alpha_N \xi)l}{(1+d^* - \alpha_N \xi l)(d^* + \alpha_N \xi l)} \cdot K_R \tag{2}$$

where a_N, an amplitude factor accounting for geometrical nonlinearity, is defined as a_N=1/(1-N_{max}/N_J^E). When this effect is negligible, a_N approaches 1, and Eq. (2) reduces to Eq. (3), referring to Fig. 9 for the definition of connection length proportions ξ_1 and ξ_2, and brace length L_0.

$$N_{cr} = \frac{1-\xi_1-\xi_2}{(1-\xi_1)\cdot\xi_2 L_0}\cdot K_R \tag{3}$$

5. Hikino and Okazaki's proposal (2013)

Hikino, Okazaki, et al. [10] discussed stability conditions of a BRB with similar boundary conditions as Koetaka et al. [9], but modelled the restrainer and connection components shown in Fig.7 (b) as rigid bodies. This model also assumes a pin at the restrainer ends, and full fixity for the lower gusset. For the case of a perpendicular member offering significant horizontal stiffness, K_H, the proposed equation becomes equivalent to Eq. (3).

$$N_{cr} = \frac{K_R}{L_1}\frac{L_1}{L_1+L_2} = \frac{K_R}{\xi l + d^*}\cdot\frac{1-2\xi-d^*}{1-\xi} = \frac{1-\xi_1-\xi_2}{(1-\xi_1)\cdot\xi_2 L_0}\cdot K_R \tag{4}$$

6. Takeuchi's proposal (2013)

Takeuchi, et al. [11] proposed stability conditions including moment-transfer capacity at the restrainer ends, M_p^r, and residual moment at the restrainer ends, M_0^r, introduced by out-of-plane drift estimated from the maximum design story drift. Moment-transfer capacity at the restrainer ends is governed by failure of the restrainer or plastic hinge formation in the neck as shown in Fig.8. Note that the neck hinging mode would also be appropriate when a collar is provided of sufficient overlap and thickness to avoid hinging in the overlap zone. When a hinge forms in the neck, M_p^r becomes a function of axial stress. This initial study assumed stiffness of the connection zones, gussets and adjacent framing are the same at both ends, generally applicable for the one-way configuration.

The potential collapse mechanisms shown in Fig. 9(a) were checked. These assume elastic rotational springs at the gusset plate ends, with the stability limit axial force, N_{lim1}, required to exceed the maximum compressive force of the core member, N_{cu}:

$$N_{lim1} = \frac{(M_p^r - M_0^r)/a_r + N_{cr}^r}{(M_p^r - M_0^r)/(a_r N_{cr}^B)+1} > N_{cu} \tag{5}$$

Here, M_p^r denotes the moment transfer capacity at the restrainer end and M_0^r denotes the initial bending moment at the restrainer ends produced by out-of-plane drift. If M_0^r exceeds M_p^r, (M_p^r - M_0^r) is taken as zero (ie no moment transfer). a_r denotes the initial imperfection at the restrainer ends and is estimated as $a_r=a_t+e+s_r+(2s_r/L_{in})\xi L_0$ (Fig. 10). N_{cr}^B denotes the global elastic buckling strength, including the effects of the connection flexural stiffness, and gusset and adjacent framing rotational stiffness.

N_{cr}^r is the connection buckling strength, where the bending-moment transfer capacity at the restrainer ends is neglected (ie cantilever buckling). Note that in the elastic range with fixed end rotations, this value can be estimated by cantilever Euler buckling $N^r_{cr}=\pi^2\gamma_J EI_B/(2\xi L_0)^2$, but that generally the base fixity has a finite spring stiffness. The governing mode is typically the asymmetric mode, which when including the effects of the rotational end springs can be expressed as:

$$N_{cr}^r = \frac{\pi^2(1-2\xi)\gamma_J EI_B}{(2\xi L_0)^2}\cdot\frac{{}_{\xi}\kappa_{Rg}}{{}_{\xi}\kappa_{Rg}+24/\pi^2} \tag{6}$$

where ξL_0 is the connection length (distance from end of restrainer to column/beam flange) and ${}_{\xi}\kappa_{Rg}$ is the normalized rotational stiffness of the connection outer ends, incorporating both the adjacent framing rotational stiffness (which depends on the brace angle), and additional rotational stiffness of the gusset due to supplementary

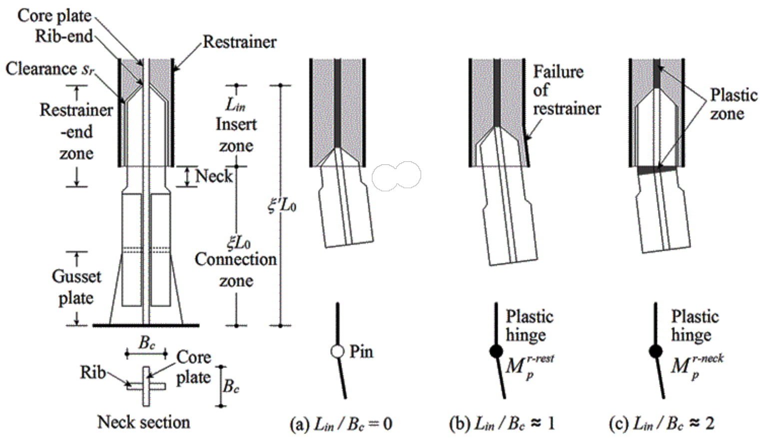

Fig. 8 – Moment transfer capacity at restrainer end[11]

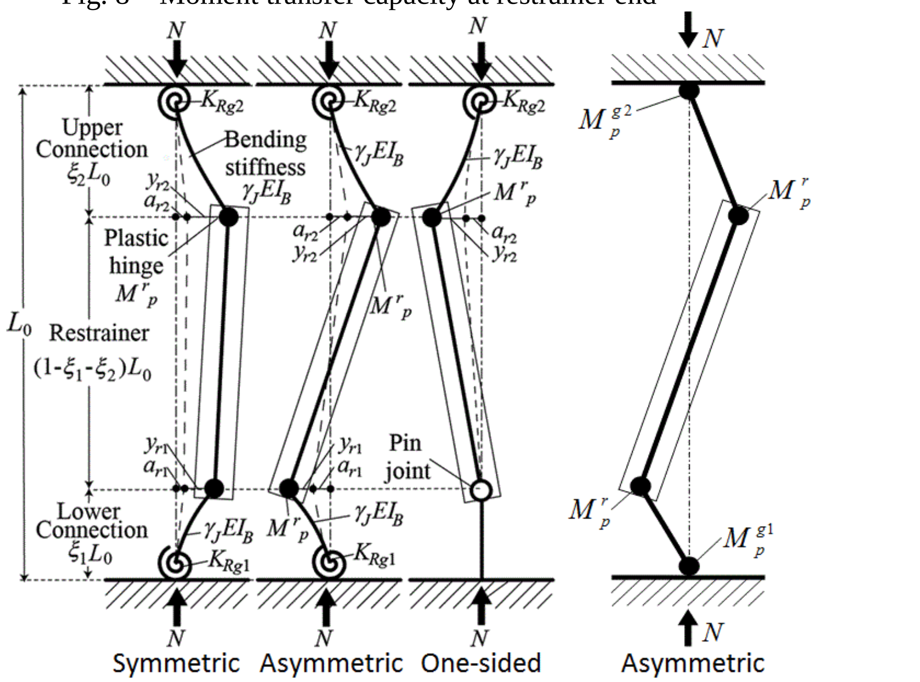

(a) Elastic spring at Gusset (N_{lim1}) (b) Plastic hinge at Gusset (N_{lim2})

Fig. 9 – Collapse mechanisms assumed by Takeuchi[11]

stiffeners and weld configuration:

$$ {}_{\xi}\kappa_{Rg} = \frac{K_{Rg}\xi L_0}{\gamma_J EI_B} \tag{7}$$

K_{Rg} is the rotational stiffness of the gusset plate. In the elasto-plastic range, $N_{cr}{}^r$ can be evaluated by substituting the equivalent slenderness ratio, given in Equation (8), into the various elasto-plastic design column curves.

$$ \lambda_r = \frac{2\xi L_0}{i_c} \cdot \sqrt{\frac{{}_{\xi}\kappa_{Rg} + 24/\pi^2}{(1-2\xi)_{\xi}\kappa_{Rg}}} \tag{8}$$

Here, i_c is the radius of gyration in the connection zone.

Note that Eq. (5) reduces to simple cantilever buckling (N_{lim1}=$N_{cr}{}^r$) if there is no moment transfer, ($M_p{}^r$ - $M_0{}^r$)→0. Likewise, Eq. (5) reduces to global pin-pin elastic buckling (N_{lim1}=$N_{cr}{}^B$) if there is full restrainer moment continuity, $M_p{}^r$→∞, and low gusset/adjacent framing rotational stiffness, $\gamma_J EI_B$→0, which produces $N_{cr}{}^r$→0.

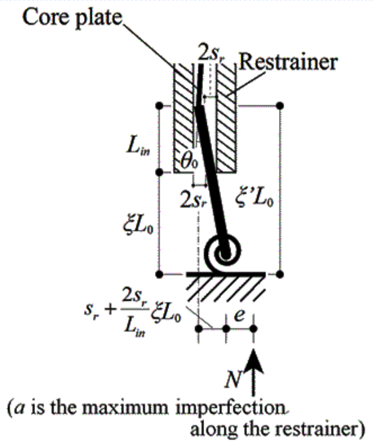

Fig. 10 Initial imperfection

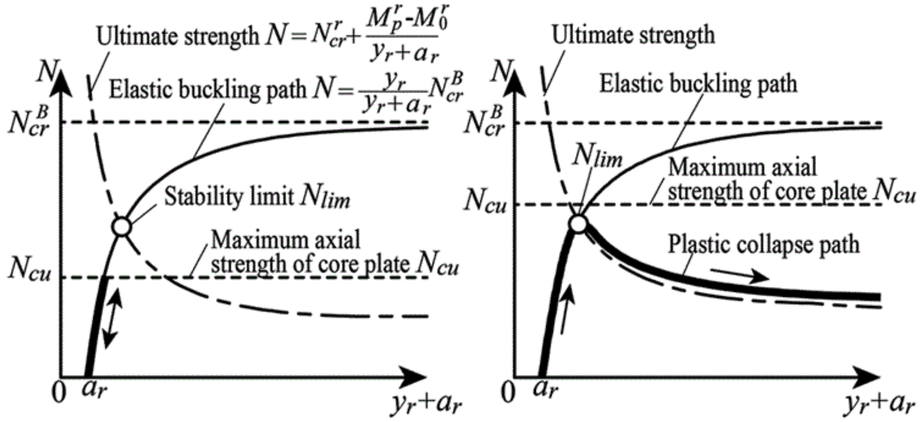

(a) Stable (N_{cu} < stability limit) (b) Unstable (N_{cu} > stability limit)

Fig.11 Stability concepts and limits

Similar to Eq. (5), but assuming that plastic hinges also form at the gusset plates as shown in Fig. 9(b), the expected limit axial force, N_{lim2}, is proposed as follows.

$$N_{lim2} = \frac{\left[\left\{(1-2\xi)M_p^g - M_0^r\right\} + \left(M_p^r - M_0^r\right)\right] / a_r}{\left[\left\{(1-2\xi)M_p^g - M_0^r\right\} + \left(M_p^r - M_0^r\right)\right] / (a_r N_{cr}^B) + 1} > N_{cu}, \tag{9}$$

where M_p^g is the plastic bending strength of the gusset plate including the axial force effect. $[(1\text{-}2\xi)M_p^g - M_0^r]$ or $[M_p^r - M_0^r]$ should be taken as zero if the difference is negative.

The smaller of the two limit forces obtained from Equations (5) and (9) becomes the limiting axial force, N_{lim}, and the BRB is considered to be stable where N_{lim} is larger than the maximum compressive force of the core, N_{cu}. These equations have been derived from the intersection of the elastic buckling path and ultimate strength curve as shown in Fig.11. The elastic buckling path can be defined as follows:

$$N = \frac{y_r}{y_r + a_r} N_{cr}^B, \tag{10}$$

where y_r denotes out-of-plane deformation at restrainer ends.

For the chevron configuration, the upper beam connection is far less stiff than the lower beam/column connection. The above equations are only applicable for symmetric stiffness conditions, where the connection length ratio, ξ, and the normalized rotational stiffness, $_\xi\kappa_{Rg}$, are the same at both ends. The upper beam loses stiffness due to both decreased rotational restraint, relying more on the torsional rotation of the connected beam, and increased connection length. The length of the upper connection, $\xi_2 L_0$, is measured from the beam centroid, while the rotational stiffness is expressed by the following Equation (11).

$$K_{Rg2} = \frac{1}{(1/K_{Rb}) + (1/K'_{Rg2})} \tag{11}$$

$$_\xi\kappa_{Rg1} = \frac{K_{Rg1}\xi_1 L_0}{\gamma_J E I_B}, \quad _\xi\kappa_{Rg2} = \frac{K_{Rg2}\xi_2 L_0}{\gamma_J E I_B} \tag{12}$$

Here, K_{Rb} is the rotational stiffness of the beam about the brace major axis with the brace bending in the out-of-plane direction, and K'_{Rg2} is the rotational stiffness of the upper gusset plate. When the rotational stiffness of the lower gusset plate at the column–beam joint is defined as K_{Rg1}, the normalized rotational stiffness at both ends can be defined as Eq. (12).

In such asymmetrical chevron configurations, Takeuchi et al.[12] gives the ultimate strength in the same formulation as for the symmetrical stiffness case:

$$N_{lim1} = \frac{(M_p^r - M_0^r)/a_r + N_{cr}^r}{(M_p^r - M_0^r)/(a_r N_{cr}^B) + 1} > N_{cu} \tag{5}$$

N_{cr}^r can be obtained using the equivalent slenderness ratio, given as follows:

$$N_{cr}^{r}=\frac{\pi^{2}\gamma_{J}EI_{B}}{(2L_{0})^{2}}\cdot\frac{C_{2}}{C_{1}},\quad \lambda_{r}=\frac{2L_{0}}{i_{c}}\cdot\sqrt{\frac{C_{1}}{C_{2}}}\ (Asymmetrical\ mode)\quad ,$$

$$C_{2}=\frac{{}_{\xi}\kappa_{Rg1}}{\xi_{1}^{3}\left({}_{\xi}\kappa_{Rg1}+3\right)}+\frac{{}_{\xi}\kappa_{Rg2}}{\xi_{2}^{3}\left({}_{\xi}\kappa_{Rg2}+3\right)}\quad C_{1}=\frac{\left({}_{\xi}\kappa_{Rg1}+24/\pi^{2}\right)\left(1+\xi_{1}-\xi_{2}\right)}{\xi_{1}\left(1-\xi_{1}-\xi_{2}\right)\left({}_{\xi}\kappa_{Rg1}+3\right)}+\frac{\left({}_{\xi}\kappa_{Rg2}+24/\pi^{2}\right)\left(1+\xi_{2}-\xi_{1}\right)}{\xi_{2}\left(1-\xi_{1}-\xi_{2}\right)\left({}_{\xi}\kappa_{Rg2}+3\right)}\qquad (13)$$

$$N_{cr}^{r}=\frac{\pi^{2}\gamma_{J}EI_{B}}{(2L_{0})^{2}}\cdot\frac{1-\xi_{1}-\xi_{2}}{1-\xi_{1}}\cdot\frac{{}_{\xi}\kappa_{Rg2}}{{}_{\xi}\kappa_{Rg2}+24/\pi^{2}},\quad \lambda_{r}=\frac{2\xi_{2}L_{0}}{i_{c}}\sqrt{\frac{\left(1-\xi_{1}\right)\left({}_{\xi}\kappa_{Rg2}+24/\pi^{2}\right)}{\left(1-\xi_{1}-\xi_{2}\right){}_{\xi}\kappa_{Rg2}}}\ (One-sided\ mode)\qquad (14)$$

Furthermore, the stability limit with plastic hinges at the gusset plates, N_{lim2}, can be expressed as follows:

$$N_{\lim 2}=\frac{\left(M_{p}^{r}-M_{0}^{r}+C_{3}\right)/a_{r}}{\left(M_{p}^{r}-M_{0}^{r}+C_{3}\right)/\left(a_{r}N_{cr}^{B}\right)+1},\quad C_{3}=\left(\frac{M_{p}^{g1}-M_{0}^{r}}{\xi_{1}}+\frac{M_{p}^{g2}-M_{0}^{r}}{\xi_{2}}\right)\frac{1}{1/\xi_{1}+1/\xi_{2}+4/\left(1-\xi_{1}-\xi_{2}\right)}$$

$$(Asymmetrical\ mode)\qquad (15)$$

$$N_{\lim 2}=\frac{\left[\left(1-\xi_{1}-\xi_{2}\right)\left(M_{p}^{g2}-M_{0}^{r}\right)/\left(1-\xi_{1}\right)+M_{p}^{r}-M_{0}^{r}\right]/a_{r}}{\left[\left(1-\xi_{1}-\xi_{2}\right)\left(M_{p}^{g2}-M_{0}^{r}\right)/\left(1-\xi_{1}\right)+M_{p}^{r}-M_{0}^{r}\right]/\left(a_{r}N_{cr}^{B}\right)+1}\quad (One-sided\ mode)\qquad (16)$$

It can easily be confirmed that Eq. (13) and Eq. (15) reduce to Eq. (8) and Eq. (9), respectively, when applying symmetry conditions $\xi_1=\xi_2=\xi$ and ${}_{\xi}\kappa_{Rg1}={}_{\xi}\kappa_{Rg2}={}_{\xi}\kappa_{Rg}$. When the moment transfer capacity $M_p{}^r=0$ and ${}_{\xi}\kappa_{Rg}$ is infinite, Eq. (6) gives the same criteria as Eq. (1) by Koetaka et al. When ${}_{\xi}\kappa_{Rg}$ is relatively small, Eq. (14) and Eq. (12) gives the same criteria as Eq. (2). Eq. (14) can alternatively be expressed as:

$$N_{cr}=\frac{\pi^{2}\gamma_{J}EI_{B}}{(2\xi_{2}L_{0})^{2}}\cdot\frac{\left(1-\xi_{1}-\xi_{2}\right){}_{\xi}\kappa_{Rg2}}{\left(1-\xi_{1}\right)\left({}_{\xi}\kappa_{Rg2}+24/\pi^{2}\right)}\rightarrow\frac{\pi^{4}}{96}\cdot\frac{K_{Rg2}}{\xi_{2}L_{0}}\cdot\frac{1-\xi_{1}-\xi_{2}}{1-\xi_{1}}\approx\frac{K_{Rg2}}{\xi_{2}L_{0}}\cdot\frac{1-\xi_{1}-\xi_{2}}{1-\xi_{1}}$$

This is the same criteria proposed by Eq. (3) by Koetaka et al. and Okazaki et al. (Eq. (4)). When, $\gamma_J EI_B$ is very small and $M_p{}^r$ is strong enough, Eq. (5) approaches $N_{lim}=N_{cr}{}^B$ which is global elastic buckling including connections. As above, Takeuchi's equation set [11], [12] covers all the past proposals.

7. Estimation of connection end rigidity (${}_{\xi}\kappa_{Rg}$)

Although the generalized stability evaluation equation set is established, an analytical method of estimating of each stiffness component is not clear. In the following discussion, simplified methods for some relevant connection details are introduced.

Normalized rotational spring ${}_{\xi}\kappa_{Rg}$ values for beam-column connections were evaluated using FEM analysis [14] and the results shown in Fig. 12. This figure indicates that a simplified method proposed by Kinoshita [15] is close to FEM results with rigid beam/column conditions. However, when beam/column deformation is considered, Kinoshita's method is not conservative. In general, gusset plates with low stiffness (Fig. 4(a)) give ${}_{\xi}\kappa_{Rg}$ values of around 0.2, and those with high stiffness (Fig. 4(b)) gives ${}_{\xi}\kappa_{Rg}$ values of around 1.0.

The influence of the rotational spring stiffness on the equivalent slenderness (Eq. (8)), and hence equivalent effective length is marked. For the case of a pin at the restrainer end, the low and high stiffness gussets produce equivalent effective lengths of 9 and 5, respectively, while the Tsai and Nakamura et al. [8] method proposes an effective length of 2, albeit with a longer L_0, dependent on beam and column sizes.

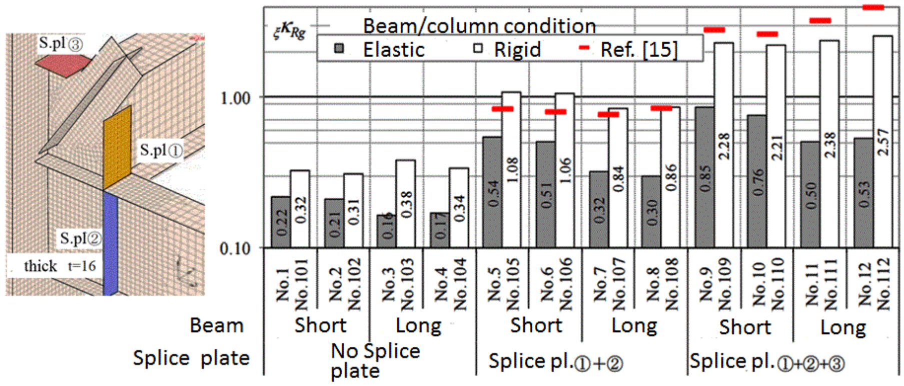

Fig.12 $_{\xi}\kappa_{Rg}$ values for beam-column connections

The normalized rotational spring stiffness, $_{\xi}\kappa_{Rg2}$, for the chevron configuration upper (beam) connection was also analysed using FEM [16], as shown in Fig. 13. The figure indicates that the rotational stiffness falls between $_{\xi}\kappa_{Rg2}$=006~0.2 if perpendicular secondary beams have nominal pin connections. With fixed secondary beams of 0.5~0.7 times the depth of the primary beam and a high stiffness gusset, rotational stiffness increases to $_{\xi}\kappa_{Rg2}$ =0.4~0.6.

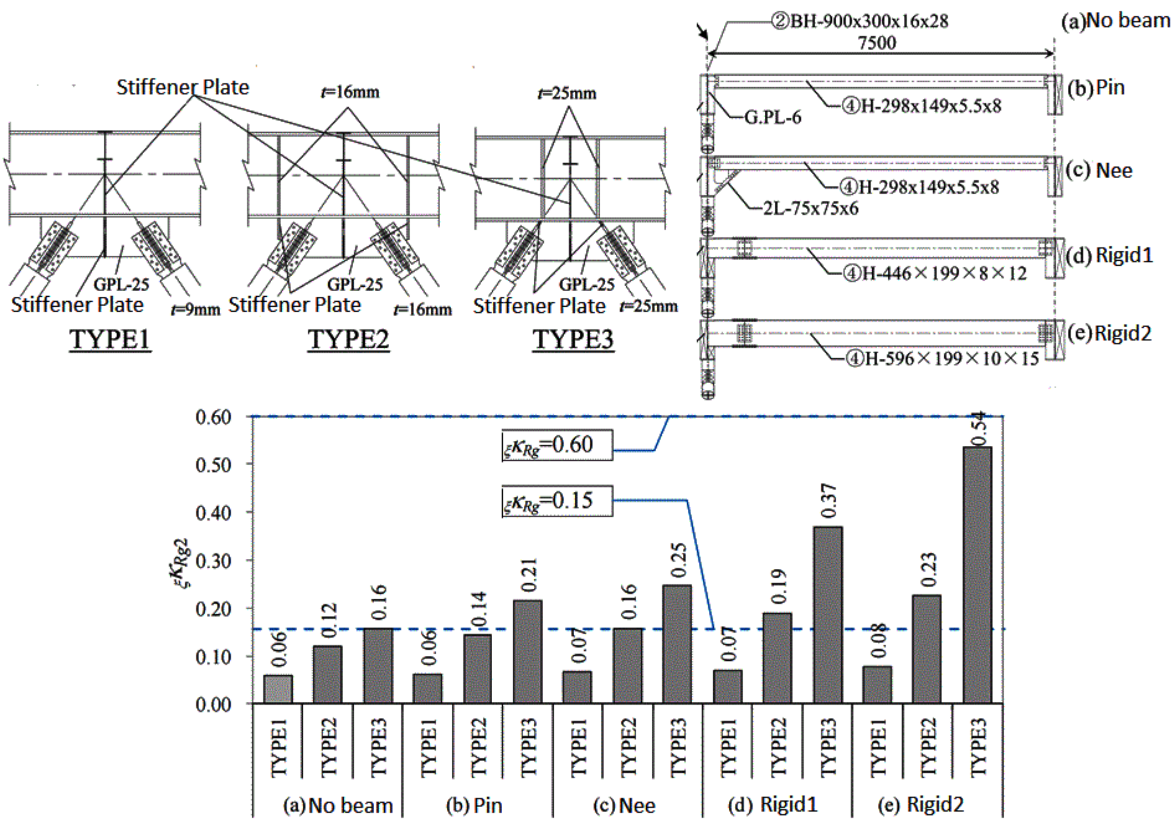

Fig.13 $_{\xi}\kappa_{Rg2}$ values for beam-side connections in chevron configurations

8. Position of the upper ends for stability evaluation

In Takeuchi et al. [12], the position of the rotational spring at the upper (beam) connection of chevron frames is also discussed, concluding that Model-3 in Fig. 14 can be used for K_{Rb}/K_{Rg2}'>10, and Model-2 can be used for K_{Rb}/K_{Rg2}'>ξ_2/ξ_g-1≈0.5~0.8. Fig. 15 shows K_{Rb}/K_{Rg2}' corresponding to the Fig. 13 FEM analysis results. Generally, the gusset point of rotation can be taken from the bottom flange of the main beam (Model-2) for Type

1 and 2 gussets (Fig. 13). For Type 3 gussets, which feature full depth edge stiffeners, the beam centroid should be assumed as the point of rotation, but in this case the rotational stiffness $_{\xi}K_{Rg2}$ itself is quite large.

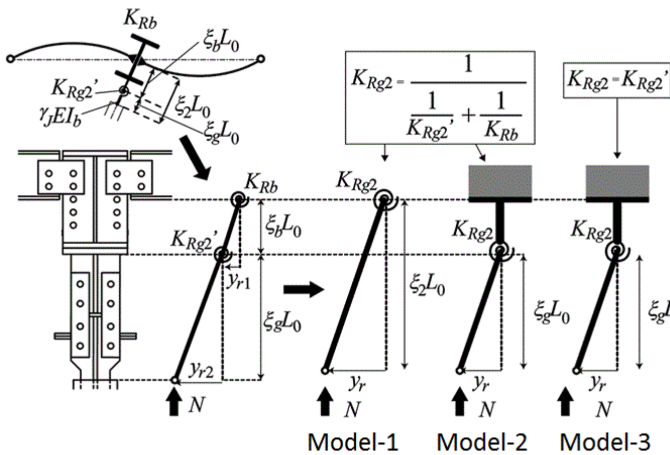

Fig.14 Position of the upper end in chevron configurations

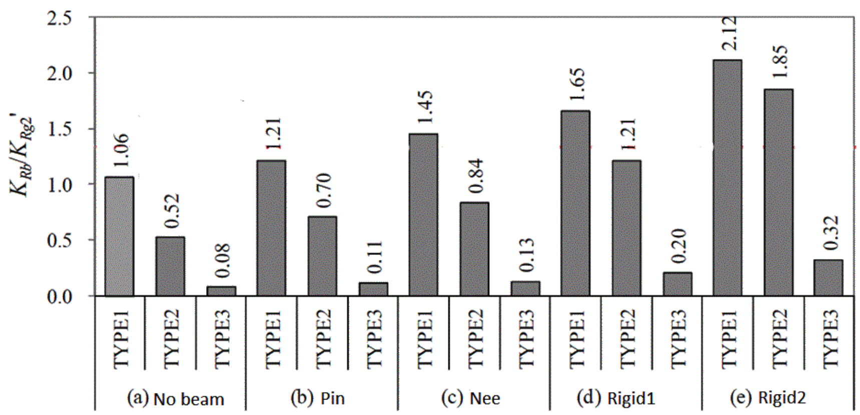

Fig.15 K_{Rb}/K_{Rg2}' values for beam-side connections in chevron configurations

9. Estimation of global elastic buckling strength of a BRB (N_{cr}^{B})

The global elastic buckling strength of a BRB, N_{cr}^{B}, including the effects of the connection zone's bending stiffness and the gusset plate's rotational stiffness, can be estimated from numerical analysis, by using the model shown in Fig. 16, or by using the following equations. For chevron configuration, K_{Rg} = min[K_{Rg1}, K_{Rg2}], and ξ = max[ξ_1, ξ_2] can be used.

$$N_{cr}^{B} = \alpha^2 EI \tag{17}$$

where, α is the value satisfying the following equations.

$$\alpha^2 (EI_B)^2 S_1 C_4 + \alpha EI_B \left(K_{Rr} S_1 S_4 - \frac{K_{Rg} + K_{Rr}}{\sqrt{\gamma_J}} C_1 C_4 \right) - K_{Rg} K_{Rr} \left(\frac{1}{\gamma_J} S_1 C_4 + \frac{1}{\sqrt{\gamma_J}} C_1 S_4 \right) = 0 \quad (Symmetric\,Mode)$$

$$\alpha^3 (EI_B)^2 L_0 S_1 S_4 - \alpha^2 EI_B L_0 \left(K_{Rr} S_1 C_4 + \frac{K_{Rg} + K_{Rr}}{\sqrt{\gamma_J}} C_1 S_4 \right) + 2\alpha EI_B K_{Rg} S_1 S_4 + \alpha K_{Rg} K_{Rr} L_0 \left(\frac{1}{\sqrt{\gamma_J}} C_1 C_4 - \frac{1}{\gamma_J} S_1 S_4 \right) - 2K_{Rg} K_{Rr} \left(S_1 C_4 + \frac{1}{\sqrt{\gamma_J}} C_1 S_4 \right) = 0$$

$(Asymmetric\,Mode)$

$$S_1 = \sin \frac{\alpha}{\sqrt{\gamma_J}} \xi L_0,\; C_1 = \cos \frac{\alpha}{\sqrt{\gamma_J}} \xi L_0,\; S_4 = \sin \alpha L_0 \left(\frac{1}{2} - \xi \right),\; C_4 = \cos \alpha L_0 \left(\frac{1}{2} - \xi \right) \tag{18}$$

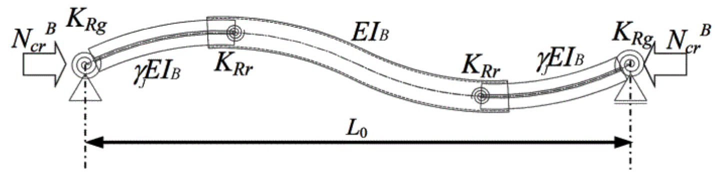

Fig. 16 Buckling mode including springs

When K_{Rr} is infinity and $\gamma_J = 1$, the solution approaches the simpler approximate formula in ref. [11].

$$N_{cr}^B = \frac{4\pi^2 EI_B}{L_0{}^2} \frac{{}_L\kappa_{Rg}^2 + 10{}_L\kappa_{Rg} + 16}{{}_L\kappa_{Rg}^2 + 14{}_L\kappa_{Rg} + 64} \tag{19}$$

where, ${}_L\kappa_{Rg} = \dfrac{K_{Rg}L_0}{EI_B}$. Note that N^B_{cr} becomes $\pi^2 EI_B/L_0{}^2$ when ${}_L\kappa_{Rg}$=0, and N^B_{cr} =$4\pi^2 EI_B/L_0{}^2$ when ${}_L\kappa_{Rg}$=∞.

10. Estimation of the bending moment produced by out-of-plane drift ($M_0{}^r$)

The initial bending moment $M_0{}^r$ at the restrainer ends produced by out-of-plane drift can be estimated from numerical analysis using the model as shown in Fig. 17 or by using the following equation. For the chevron configuration, ${}_\xi\kappa_{Rg}$ = max[${}_\xi\kappa_{Rg1}$, ${}_\xi\kappa_{Rg2}$], and ξ'= min[ξ'_1, ξ'_2] can be taken.

$$M_0^r = (1-2\xi)\left\{\frac{\delta_0}{L_0} - \frac{2s_r}{L_{in}}(1-2\xi)\right\}\cdot\frac{EI_B}{L_0}\cdot\frac{6\gamma_J}{2\xi'(3-6\xi'+4\xi'^2)+\gamma(1-2\xi')^3+\dfrac{6\xi}{{}_\xi\kappa_{Rg}}+\dfrac{6\gamma_J(1-2\xi')^2}{{}_L\kappa_{Rr}}} \geq 0 \tag{20}$$

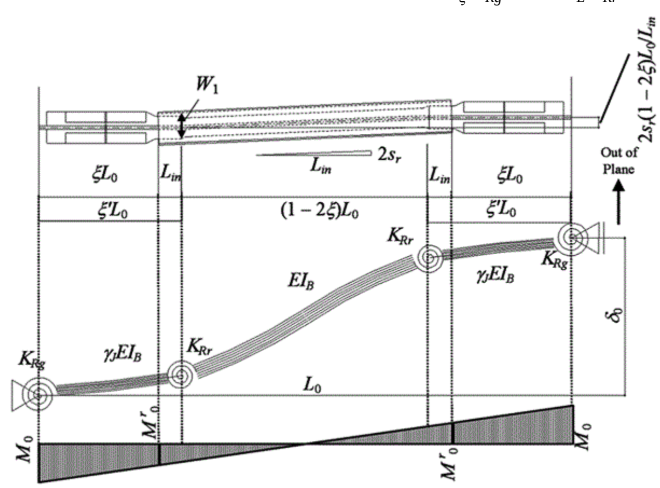

Fig. 17 Bending moment produced by out-of-plane drift

$$\text{where,}\quad {}_\xi\kappa_{Rg} = \frac{K_{Rg}\xi L_0}{\gamma_J EI_B}\ ,\ {}_L\kappa_{Rr} = \frac{K_{Rr}L_0}{EI_B}\ ,\ \xi' = \xi + \frac{L_{in}}{L_0} \tag{21}$$

K_{Rg} is the rotational spring at the gusset plates and K_{Rr} is the rotational spring at the restrainer ends. When $K_{Rr}\rightarrow\infty$, $EI_B/L_0\rightarrow\infty$, γ= 1 and ξ'= ξ, this equation approaches the simpler formulas from the previous study (Eq. (31) in Reference [11]):

$$M_0^r = (1-2\xi)\left\{\frac{\delta_0}{L_0} - \frac{2s_r}{L_{in}}(1-2\xi)\right\}K_{Rg} \geq 0 \tag{22}$$

$M_0{}^r$ becomes zero when $\dfrac{\delta_0}{L_0} \leq \dfrac{2s_r}{L_{in}}(1-2\xi)$, from Equations (20) and (22).

Reflecting on the proposed equations, the following process can be applied in practice to ensure BRB stability:

For the one-way configuration shown in Fig. 5(a), (Bolted and welded connections):

1. Estimate the normalized gusset rotational spring, ${}_{\xi}\kappa_{Rg}$, according to Section 7, and then estimate $N_{cr}{}^{r}$ by applying the equivalent slenderness ratio from Eq. (8) into column design curves.
2. Estimate the initial imperfection at the restrainer ends, a_r (Fig. 10), the global elastic buckling strength, $N_{cr}{}^{B}$ (Section 9), and the initial bending moment at the restrainer ends due to out-of-plane drift, $M_0{}^{r}$ (Section 10).
3. Estimate the restrainer end moment-transfer capacity, $M_p{}^{r}$, if any, and the plastic gusset bending strength, $M_p{}^{g}$, including axial actions. To estimate $M_p{}^{r}$, specific equations for each restrainer configuration need to be established. Refer to [11] for equations applicable to mortar-filled steel-tube BRBs with cruciform inserts.
4. Calculate N_{lim1} by Eq. (5) and N_{lim2} by Eq. (9). The stability limit, N_{lim}, is the smaller of N_{lim1} and N_{lim2}.
5. If N_{lim} is larger than the expected compressive force of the core, N_{cu}, BRB stability is secured. If not, increase K_{Rb}, $K'_{Rg,}$ or $M_p{}^{r}$ and repeat steps 1 to 5.

For the chevron configuration shown in Fig. 5(b), (Bolted and welded connections):

1. Estimate the normalized rotational spring stiffness at the upper (beam) side, ${}_{\xi}\kappa_{Rg2}$ (Section 7), then estimate $N_{cr}{}^{r}$ by applying the equivalent slenderness ratio from Eq. (13) or Eq. (14) into column design curves.
2. Estimate upper a_r from Fig.10, $N_{cr}{}^{B}$ (Section 9), and $M_0{}^{r}$ (Section 10).
3. If moment transfer capacity is expected, estimate $M_p{}^{r}$ and $M_p{}^{g}$, including the axial actions.
4. Calculate N_{lim1} by Eq. (5) and N_{lim2} by Eq. (15) and Eq. (16). The stability limit, N_{lim}, is the smaller of N_{lim1} and N_{lim2}.
5. If N_{lim} is larger than expected compressive force of the core, N_{cu}, BRB stability is secured. If not, increase K_{Rb}, $K'_{Rg,}$ or $M_p{}^{r}$ and repeat steps 1 to 5.

For the pinned connection shown in Fig. 3(c), buckling behaviour depends on which direction the pin is orientated. If the pin joint transfers out-of-plane bending moment, use the process for the bolted connections. Otherwise, assuming that pin fully releases out-of-plane moment, use the following process:

1. Estimate normalized rotational spring ${}_{\xi}\kappa_{Rg}$ (one-way) or ${}_{\xi}\kappa_{Rg1}$, ${}_{\xi}\kappa_{Rg2}$ (chevron) according to Section 7, and then estimate $N_{cr}{}^{r}$ by applying the equivalent slenderness ratio from Eq. (8) (one-way), Eq. (13) or Eq. (14) (chevron) into design column curves. ξL_0 can be estimated as the distance between the beam/column flange and pin point of rotation.
2. Estimate $M_p{}^{g}$, including axial actions and take $M_p{}^{r} = M_0{}^{r} = 0$.
3. Calculate N_{lim1} by Eq. (5) and N_{lim2} by Eq. (9) (one-way) or Eq. (15) (chevron). The stability limit, N_{lim}, is the smaller of N_{lim1} and N_{lim2}.
4. If N_{lim} is larger than expected compressive force of the core, N_{cu}, BRB stability is secured. If not, increase K_{Rb}, K'_{Rg} and repeat steps 1 to 5.

These equations can also be readily formulated into design charts, refer to [17] for an example.

In the above procedures, other sources of premature failure such as core bulging through the restrainer wall and fracture of the adjacent framing are assumed to be suppressed. Recent research into these mechanisms and recommended design procedures are reviewed in a companion paper [18].

12. Conclusions

Previously proposed BRB stability criteria are reviewed and compared, and a unified concept explaining all of those proposals are introduced, followed by a simplified approach for practical design. In summary:

1) The proposals by Koetaka, Inoue et al. and Hikono, Okazaki et al. are confirmed to be equivalent criteria as Takeuchi's proposal when the moment transfer capacity at the restrainer ends is neglected.

2) The criteria indicated by Tsai, Nakamura et al. can underestimate the connection buckling strength when comparing the condition of no moment transfer capacity at the restrainer ends.

3) A unified stability criteria covering all the conditions is proposed, based on Takeuchi's proposals for both the one-way and chevron configurations.

Acknowledgements

The authors would like to acknowledge the support of Nippon Steel and Sumikin Engineering Co. Ltd, Nikken Sekkei Co. Ltd, and great contributions of Dr. Yoshinao Konishi, Dr. Hitoshi Ozaki, Dr. Fatih Sutcu and Miss. Saki Mihara for this study.

References

[1] Fujimoto M, Wada A, Saeki E, Takeuchi T, Watanabe A (1990): Development of Unbonded Brace. *Quarterly Column*, **115**, 91-96.

[2] Architectural Institute of Japan (2009): Recommendations for stability design of steel structures, Sec. 3.5 Buckling-restrained Braces. 74–79.

[3] Architectural Institute of Japan (2012): Recommended provisions for seismic damping systems applied to steel structures, Sec. 3 Buckling-restrained Braces. 24–59.

[4] AISC 341 (2010): Seismic provisions for structural steel buildings, F4: Buckling-Restrained Braced Frames.

[5] Architectural Institute of Japan (2013): Stability problems of steel structures, Sec. 2 Stability assessment of Buckling-restrained Braces including connections. 19–38.

[6] Wigle VR, Fahnestock LA (2010): Buckling-restrained braced frame connection performance. *Journal of Constructional Steel Research*, **66**, 65-74.

[7] Lin PC, Tsai KC, Wang KJ, Yu YJ, Wei CY, Wu AC, Tsai CY, Lin CH, Chen JC, Schellenberg AH, Mahin SA, Roeder CW (2012): Seismic design and hybrid tests of a full-scale three-story buckling-restrained braced frame using welded end connections and thin profile, *Earthquake Engineering & Structural Dynamics*, **41 (**5), 1001–1020.

[8] Tsai KC, Huang YC, Weng CS, Shirai T, Nakamura H (2002): Experimental tests of large scale buckling restrained braces and frames. *Proceedings, 2nd Passive Control Symposium*, Tokyo Institute of Technology.

[9] Koetaka Y, Kinoshita T, Inoue K, Iitani K (2008): Criteria of buckling-restrained braces to prevent out-of-plane Buckling. *Proceedings of 14th World Conference on Earthquake Engineering*.

[10] Hikno T, Okazaki T, Kajiwara K, Nakashima M (2013): Out-of-Plane stability of buckling-restrained braces placed in chevron arrangement. *Journal of Structural Engineering, ASCE,* **139** (11), DOI:10.1061/(ASCE)ST.1943-641X.0000767.

[11] Takeuchi T, Ozaki H, Matsui R, Sutcu F (2013): Out-of-plane Stability of Buckling -Restrained Braces including Moment Transfer Capacity. *Earthquake Engineering & Structural Dynamics*, DOI:10.1002/eqe.2376.

[12] Takeuchi T, Matsui R, Mihara S (2016): Out-of-plane stability assessment of buckling-restrained braces including connections with chevron configuration. *Earthquake Engineering & Structural Dynamics*, DOI: 10.1002/eqe.2724.

[13] Bruneau M, Uang CM, Sabelli RSE (2011): *Ductile design of Steel Structures, Chap.11, Ductile design of Buckling-restrained frames*. McGraw-Hill, 2nd edition.

[14] Ida M, Takeuchi T, Matsui R, Konishi Y, et al (2013): Stability Assessment of Buckling Restrained Braces Taking Connections into Account (Part.2 Evaluation of Rotational Stiffness of Brace Connections). *Proceedings of AIJ annual meeting, Structure-III*, 22624, 1247-1248. (in Japanese)

[15] Kinoshita T, Koetaka Y, Inoue I, Iitani K (2008): Out-of-plane stiffness and yield strength of cruciform connections for buckling-restrained braces. *AIJ Journal of structural and constructional engineering*, **73** (632), 1865-1873. DOI.org/10.3130/aijs.73.1865. (in Japanese)

[16] Ohyama S, Takeuchi T, Matsui R, Konishi Y, et al. (2015): Stability Assessment of Buckling Restrained Braces Taking Connections into Account, (Part.15 Calculation Methods of Rotational Stiffness of Brace Connections in Chevron Configuration). *Proceedings of AIJ annual meeting, Structure-III*, 22548, 1095-1096. (in Japanese)

[17] Ozaki H, Konishi Y, Matsui R, Takeuchi T (2014): Out-of-plane stability factors for diagonally installed buckling restrained braces. *J. Struct Constr Eng., AIJ,* **79** (706) 1919-1929. (in Japanese)

[18] Sitler B, MacRae G, Takeuchi T, Matsui R, Westeneng B, Jones A (20169: BRB performance issues. *16th World Conference on Earthquake Engineering*.